JOURNAL OF AERONAUTICS AND SPACE TECHNOLOGIES
(ISSN : 1304-0448)
July 2019 Volume 12 Number 2
www.jast.hho.edu.tr

Research Article

Peridynamic Solution of The Steady State Heat Conduction Problem in Plates with İnsulated Cracks

Mehmet DÖRDÜNCÜ[1]

[1]*Department of Mechanical Engineering, Erciyes University, Kayseri, Turkey*, dorduncu@erciyes.edu.tr , http://orcid.org/0000-0003-4028-4581

Article Info

Received: *April 7, 2019*
Accepted: *May 26, 2019*
Online: *July 12, 2019*

Keywords: Peridynamic Differential Operator, Nonlocal Models, Crack, Heat Conduction.

Abstract

This paper presents the steady-state heat conduction analysis in plates with insulated cracks using peridynamic differential operator (PDDO). The PDDO converts the local differentiation to nonlocal integration. Since the PDDO permits differentiation through integration, the equilibrium equations remain valid in the presence of discontinuities such as cracks. The governing equations of the steady state heat equation and boundary conditions were solved by employing the PDDO. The robustness of the PDDO was assessed by considering a plate without cracks under different boundary conditions. The influence of the insulated cracks on the temperature and heat flux distributions was investigated. It was observed that heat flux concentrations developed in the vicinity of the crack tips.

To Cite This Article: M. Dorduncu, "Peridynamic Solution of The Steady State Heat Conduction Problem in Plates with İnsulated Cracks" Journal of Aeronautics and Space Technologies, Vol. 12, No. 2, pp. 145-155, Jul. 2019.

Yalıtılmış Çatlaklı Levhalarda Kararlı Hal Isı İletimi Probleminin Peridinamik Çözümü

Makale Bilgisi

Geliş: *7 Nisan 2019*
Kabul: *26 Mayıs 2019*
Yayın: *12 Temmuz 2019*

Anahtar Kelimeler: Peridinamik Türev Operatörü, Yerel Olmayan Modeller, Çatlak, Isı İletimi.

Öz

Bu makale, peridinamik diferansiyel operatörü (PDDO) kullanarak yalıtımlı çatlaklara sahip plakalarda kararlı hal ısı iletim analizini sunmaktadır. PDDO, yerel olmayan türev ifadeleri, yerel olmayan integral ifadelerine dönüştürmektedir. PDDO türev alma işlemini, integrasyon yoluyla elde ettiği için, denge denklemleri çatlaklar gibi süreksizliklerin varlığında geçerliğini korumaktadır. Kararlı hal ısı denklemi ve sınır şartları, PDDO kullanılarak çözülmüştür. PDDO'nun sağlamlığı, farklı sınır koşulları altında çatlaksız bir levha göz önüne alınarak değerlendirildi. Yalıtılmış çatlakların, sıcaklık ve ısı akışı dağılımları üzerindeki etkisi incelenmiştir. Çatlak uçlarının çevresinde ısı akısı yoğunlaşmalarının geliştiği gözlenmiştir.

1. INTRODUCTION

Heat conduction problems have been extensively considered in many fields such as nuclear, military, and aerospace. Heat conduction equations are expressed in the form of differential equations which are commonly solved by employing classical numerical methods such as finite element method (FEM) and finite-difference method (FDM). Nevertheless, they may face difficulties when the solution domain involves any discontinuity such as cracks. Therefore, it is crucial to approximate the derivatives of the field variables for the accuracy of the solution of differential equations.

Numerous studies have been performed to examine the heat conduction problems for the bodies having cracks by employing the classical heat conduction models. Sih [1] carried out a heat conduction analysis in the infinite

plate with a crack by using complex variables. Chen and Chang [2-4] investigated the steady-state heat conduction problems in a plate with multiple insulated cracks using the finite element alternating method. The analytical solution to the heat conduction problems in the bodies include discontinuities becomes challenging, especially if the solution domain has complex geometries and boundary conditions. Thus, in the literature, analytical solutions and classical methods are restricted to simpler configurations.

As an alternative to the classical solution methods, the nonlocal mesh-free methods such as reproducing kernel particle method (RKPM), generalized finite difference

method (GFDM), and smoothed particle hydrodynamics (SPH) were developed [5]. Unlike local methods, such techniques take into account the nonlocal interactions between the material points located within a region of finite radius (domain of interaction). Mahan and Claro [6] developed a nonlocal model to relate the heat current obtained from Boltzmann's equation and the temperature gradient. Lebon and Grmela [7], proposed a weakly nonlocal model based on nonequilibrium thermodynamics. Gerstle et al. [8] developed a Peridynamic (PD) model for one-dimensional heat conduction problems. Bobaru and Duangpanya [9] developed a PD model of heat conduction equation and investigated domains with multiple insulated cracks. Both studies adopted the bond-based PD approach [10].

Although nonlocal meshless methods offer advantages over the local differentiation methods, they are still confronted with difficulties in the use of kernel functions and the implementation of the essential boundary conditions. Recently, Madenci et al. [11] proposed Peridynamic Differential Operator (PDDO). This operator introduces an internal parameter which defines the domain of interaction between the grid points. Also, the PDDO converts the local differentiation to its nonlocal integral form. Thus, it paves the way to obtain the solution of differential equations by providing a relationship between differentiation and integration.

This paper presents the solution of the heat conduction problems in the plates with/without cracks by using the PDDO. The present approach converts the spatial derivatives to the integral terms so that complications arising from the discontinuities appear in the temperature field can be eliminated. The influence of the parameters used in the PDDO such as grid spacing between the material points and domain of interaction (horizon) is investigated by performing a convergence study for the plate without any crack. As the cracks in the structural components may result in intensified heat flux concentrations near the crack tips leading to the catastrophic failures, the temperature and heat flux distributions of the structures should be well understood for their structural integrity. Therefore, the capability of the PDDO was demonstrated by considering three different plate configurations including insulated crack(s) under thermal and heat flux boundary conditions.

2. PERIDYNAMIC DIFFERENTIAL OPERATOR

The Peridynamic (PD) theory is a meshless nonlocal theory, which was introduced by Silling [12] and Silling et al. [13]. In the PD theory, the state of the material point $\mathbf{x}$ is influenced by other points, $\mathbf{x}'$, within a finite domain, which is named horizon $H_{\mathbf{x}}$, (Figure 1). The solution domain, *D*, consists of material points and each point has its own family members with an infinitesimally small volume. The initial relative position, $\boldsymbol{\xi}$, between the material points $\mathbf{x}$ and $\mathbf{x}'$ can be expressed as $\boldsymbol{\xi} = \mathbf{x} - \mathbf{x}'$.

As described by Madenci et al. [11], the PD Differential Operator (PDDO) can be constructed for the *M*-dimensional space by using *N*-th order Taylor series expansion as

$$\frac{\partial^{p_1+p_2+\cdots+p_N} f(\mathbf{x})}{\partial x_1^{p_1} \partial x_2^{p_2} \cdots \partial x_M^{p_N}} = \int_{H_{\mathbf{x}}} f(\mathbf{x}+\boldsymbol{\xi})\, g_N^{p_1 p_2 \cdots p_N}(\boldsymbol{\xi}) dV \qquad (1)$$

where $p_i \quad (i = 1,...,N)$ is the order of differentiation with respect to $x_i \quad (i = 1,...,M)$.

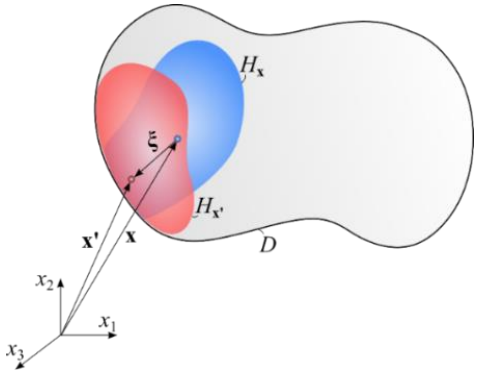


Figure 1. Interaction of peridynamic points in their families.

The PD functions, $g_N^{p_1 p_2 \cdots p_N}(\boldsymbol{\xi})$ have the orthogonality property, and they can be constructed as

$$g_N^{p_1 p_2 \cdots p_N}(\boldsymbol{\xi}) = \sum_{q_1=0}^{N} \sum_{q_2=0}^{N-q_1} \cdots \sum_{q_N=0}^{N-q_1-\cdots-q_{N-1}} a_{q_1 q_2 \cdots q_N}^{p_1 p_2 \cdots p_N} w_{q_1 q_2 \cdots q_N}(|\boldsymbol{\xi}|)\, \xi_1^{q_1} \xi_2^{q_2} \cdots \xi_M^{q_N} \qquad (2)$$

where $w_{q_1 q_2 \cdots q_N}(|\boldsymbol{\xi}|)$ express the weight functions which indicate the degree of interactions between the material points within the family.

The unknown coefficients, $a_{q_1 q_2 \cdots q_M}^{p_1 p_2 \cdots p_N}$, can be determined from the solution of

$$\sum_{q_1=0}^{N} \sum_{q_2=0}^{N-q_1} \cdots \sum_{q_N=0}^{N-q_1-\cdots-q_{N-1}} A_{(n_1 n_2 \cdots n_N)(q_1 q_2 \cdots q_N)}\, a_{q_1 q_2 \cdots q_N}^{p_1 p_2 \cdots p_N} = b_{n_1 n_2 \cdots n_N}^{p_1 p_2 \cdots p_N} \qquad (3)$$

in which $q_i = 0, ..., N$. The PD coefficient (shape) matrix, $A_{(n_1 n_2 \cdots n_N)(q_1 q_2 \cdots q_N)}$, is constructed as

$$A_{(n_1 n_2 \cdots n_N)(q_1 q_2 \cdots q_N)} = \int_{H_x} w_{q_1 q_2 \cdots q_N}(|\xi|)\ \xi_1^{n_1+q_1} \xi_2^{n_2+q_2} \cdots \xi_M^{n_N+q_N}\, dV \quad (4a)$$

and

$$b_{n_1 n_2 \cdots n_N}^{p_1 p_2 \cdots p_N} = n_1!n_2!\cdots n_N!\ \delta_{n_1 p_1}\delta_{n_2 p_2}\cdots\delta_{n_N p_N}. \quad (4b)$$

Eq. (3) can be written in the matrix form as

$$Aa=b \quad (5)$$

where A represents the PD shape matrix, a is the matrix of unknown coefficients, and b is the matrix of known coefficients. Solving for the unknown coefficients by $a=A^{-1}b$ completes the construction of PD functions.

3. TWO-DIMENSIONAL HEAT CONDUCTION EQUATION

Heat transfer processes can be written in terms of rate equations. The rate of heat conduction can be expressed for the homogeneous and isotropic solids by Fourier's law as [14]

$$\mathbf{q} = -k\nabla T \quad (6)$$

where q is the heat flux vector, T represents the temperature field . The quantity k is referred to the thermal conductivity.

In the absence of the heat generation and time, the two-dimensional steady-state heat conduction equation in the Cartesian coordinate system can be expressed in the form

$$\frac{\partial^2 T(x_1,x_2)}{\partial x_1^2} + \frac{\partial^2 T(x_1,x_2)}{\partial x_2^2} = 0 \quad (7a)$$

or

$$\nabla^2 T(x_1,x_2) = 0 \quad (7b)$$

where x_1 and x_2 are the spatial variables. Eq. (7) is also known as Laplace Equation.

4. NUMERICAL IMPLEMENTATION

The nonlocal PD form of the Laplace equation equation, Eq. (7) can be expressed by replacing the spatial derivatives of the temperature field with the PDDO as

$$\sum_{j=1}^{N_{(k)}} \mu_{(k)(j)} \Big[T(x_{1(j)},x_{2(j)}) g_2^{20}(\xi_{1(k)(j)},\xi_{2(k)(j)}) + T(x_{1(j)},x_{2(j)}) g_2^{20}(\xi_{1(k)(j)},\xi_{2(k)(j)}) \Big] A_{(j)} = 0 \quad (8)$$

where $\xi_{1(k)(j)} = x_{1(j)} - x_{1(k)}$, $\xi_{2(k)(j)} = x_{2(j)} - x_{2(k)}$, and $A_{(j)} = \Delta x_1 \Delta x_2$. The PD functions $g_2^{20}(\xi_{1(k)(j)},\xi_{2(k)(j)})$ and $g_2^{02}(\xi_{1(k)(j)},\xi_{2(k)(j)})$ are constructed by using Eq. (2) and express the second order derivative of the temperature field with respect to x_1 and x_2, respectively. The status parameter, $\mu_{(k)(j)}$, defines a crack by removing the interactions between the PD points and.can be given as

$$\mu_{(k)(j)} = \begin{cases} 1 & \text{unbroken interaction,} \\ 0 & \text{broken interaction.} \end{cases} \quad (9)$$

Similarly, the specified boundary conditions can be expressed in a general form as

$$\sum_{j=1}^{N_{(k)}} \mu_{(k)(j)} \left[\begin{matrix} T(x_{1(j)},x_{2(j)}) \times \\ g_2^{pq}(\xi_{1(k)(j)},\xi_{2(k)(j)}) A_{(j)} \end{matrix} \right] = d_{(k)} \quad (10)$$

where p and q represent the order of the differentiation with respect to x_1 and x_2, respectively. $d_{(k)}$ is the specified temperature or heat flux value.

The discretized form of the Laplace equation, Eq. (7) can be expressed as

$$F(u,b)= Lu + b =0 \quad (11)$$

where the matrix L is the coefficient matrix arising from the PD interactions between the material points, the vector u represents the PD unknowns at each material point. The vector b includes the known values of at each point.

Also, the boundary conditions can be expressed as constraint equations in the form

$$Gu + d = 0 \quad (12)$$

where the known matrix, G contains the coefficients arising from the PD differentiation , and the vector d contains the specified known values of constraint equations.

The resulting equation can then be recast as

$$\begin{bmatrix} \mathbf{L} & \mathbf{G}^T \\ \mathbf{G} & \mathbf{0} \end{bmatrix} \begin{Bmatrix} \mathbf{u} \\ \boldsymbol{\lambda} \end{Bmatrix} = - \begin{Bmatrix} \mathbf{b} \\ \mathbf{d} \end{Bmatrix} \tag{13}$$

where $\boldsymbol{\lambda}$ is the Lagrange multipliers [11].

5. RESULTS AND DISCUSSION

The validity of the present approach is demonstrated by the comparisons between the PDDO results and those from analytical solutions and ANSYS (PLANE55) predictions. The effect of the grid spacing between the material points , Δ, and horizon size ($\delta = m\Delta$) is investigated to achieve accurate results. The weight function (the degree of interaction between the material points) is specified as a Gaussian distribution in the form of

$$w(|\boldsymbol{\xi}|) = e^{-(2|\boldsymbol{\xi}|/\delta)^2} \tag{14}$$

The error between the PDDO results and analytical results is measured based on a relative error defined by

$$\varepsilon = \frac{\left\| T^A - T^{PD} \right\|}{\left\| T^A \right\|} \tag{15}$$

in which the superscripts *A* and *PD* represent the analytical and PDDO results, respectively.

5.1. Plate Without Cracks Under Temperature Boundary Conditions

The plate has the length and width of *L*= 1 cm and *W*= 1 cm as shown in Figure 2. The plate is subjected to temperature and heat flux boundary conditions as given by

$$q_{x1} = \frac{\partial T(x_1 = 0, x_2)}{\partial x_1} = 0 \tag{16a}$$

$$q_{x1} = \frac{\partial T(x_1 = W, x_2)}{\partial x_1} = 0 \tag{16b}$$

$$T(x_1, x_2 = 0) = 0 \tag{16c}$$

$$T(x_1, x_2 = L) = f(x) \tag{16d}$$

with

$$f(x_1) = \sin\left(\frac{\pi x_1}{L}\right) \tag{16e}$$

The exact solution to the Laplace equation can be written as

$$T(x_1, x_2) = A_0 x_2 + \sum_{n=1}^{\infty} A_n \cos\left(\frac{n\pi x_1}{\ell_1}\right) \sinh\left(\frac{n\pi x_2}{\ell_2}\right) \tag{17a}$$

with

$$A_0 = \frac{1}{\ell_1 \ell_2} \int_0^{\ell_1} f(x_1) dx_1 \tag{17b}$$

and

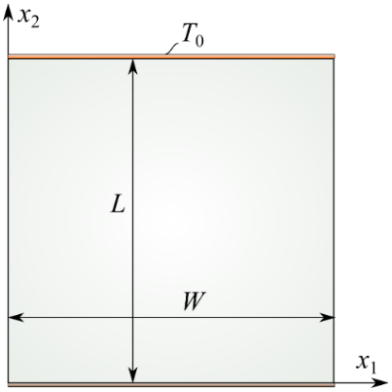


Figure 2. The plate under temperature and heat flux boundary conditions.

$$A_n = \frac{2}{\ell_1 \sinh\left(\frac{n\pi \ell_2}{\ell_1}\right)} \int_0^{\ell_1} f(x_1) \cos\left(\frac{n\pi x_1}{\ell_1}\right) dx_1 \tag{17c}$$

The convergence study is performed to understand the effect of the grid spacing between the material points, Δ and the horizon size, $\delta = m\Delta$. Thus, the plate is uniformly discretized with the grid spacings of $\Delta = \Delta x_1 = \Delta x_2 = L/50, L/75,$ and $L/100$, and the horizon/grid spacing ratio is fixed to *m*=3,4, and 5.

The relative error in the temperature predictions is determined by Eq. (15). As shown in Fig 3, the error decreases when the grid spacing is reduced. Also, the PD temperature predictions recover the local solution with decreasing the horizon size. In PD analysis, the computational time increases with increasing the horizon size; thus, it is important to use the optimal family (horizon) size for the desired computational efficiency. Based on the convergence study, the family of each point is established by the horizon size of $\delta = 3\Delta$ associated with the grid spacing of $\Delta = L/100$.

Figures 4 and 5 show the PD temperature and heat flux predictions. Also, the comparisons of the PD temperature and heat fluxes with those of anaytical and finite element analysis (FEA) are presented in Figure 6. The analytical solution is obtained by using Eq.(17) while the finite element results are produced by using PLANE55 element of ANSYS, a commercially available FEA program.

In ANSYS model, the solution domain has 3710 elements with 3844 nodes. As seen in Figs. 4 and 5, the accurate and correct temperature and heat flux distributions are successfully captured. Moreever, Figure 6 shows that the PD temperature and heat flux predictions are in good agreement with the analytical and ANSYS results.

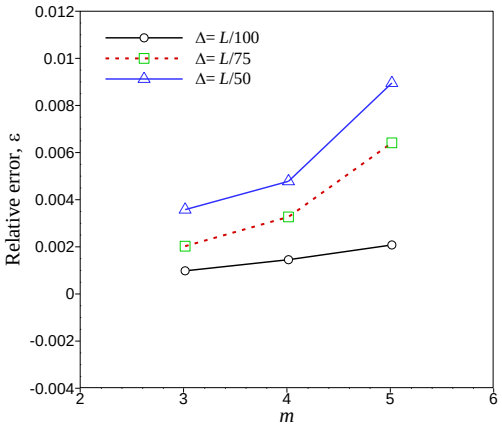


Figure 3. Convergence of the PD numerical solution.

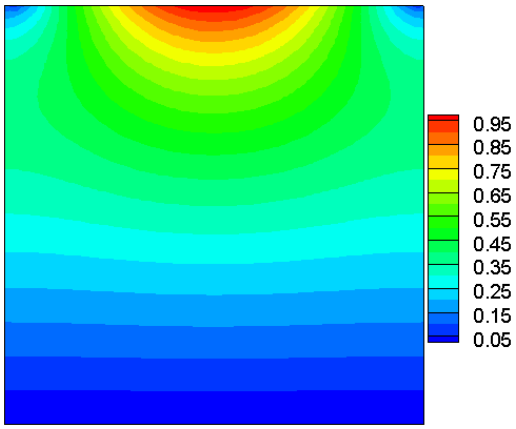


Figure 4. PD predictions for the temperature field. $T(x_1, x_2)$ (°C).

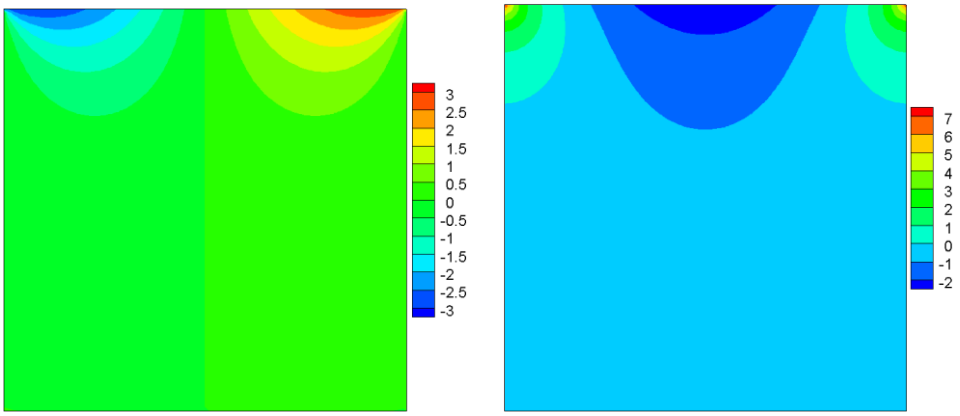


Figure 5. PD predictions for the heat flux distributions: (a) horizontal flux , $q_{x1}(x_1, x_2)$ (W/cm^2), and (b) vertical flux, $q_{x2}(x_1, x_2)$ (W/cm^2).

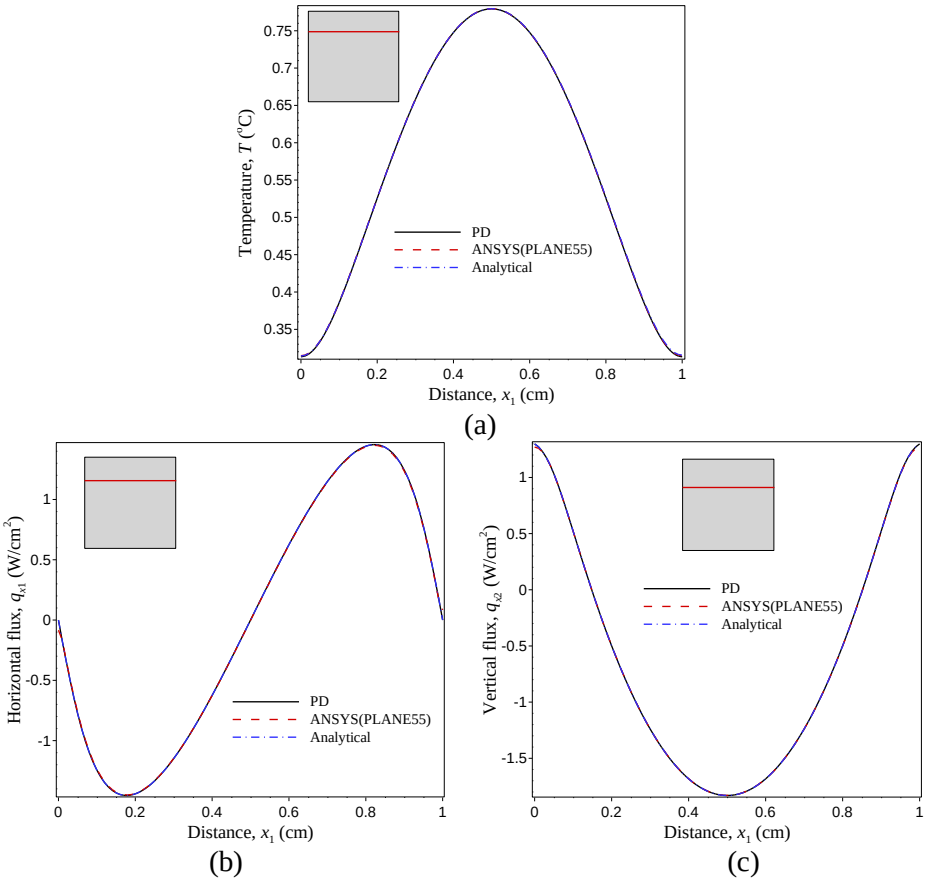


Figure 6. Comparisons of the PD temperature and heat fluxes with analytical and ANSYS results along the $x_2 = 0.9$ cm: (a) Temperature $T(x_1, x_2 = 0.9)$, (b) horizontal flux $q_{x1}(x_1, x_2 = 0.9)$, and (c) vertical flux $q_{x2}(x_1, x_2 = 0.9)$.

5.2. Plate with an İnsulated Crack Under Temperature Boundary Conditions

The plate geometry is the same as specified previously. The plate has a pre-existing insulated crack at the center with a length of 2*a*= 0.2 cm as shown in Figure 7. The plate is subjected to temperature boundary conditions along the bottom and top edges while the left and right edges are insulated as given by

$$T(x_1, x_2 = 0) = -T_0 \tag{18a}$$

$$T(x_1, x_2 = L) = T_0 \tag{18b}$$

$$q_{x1} = \frac{\partial T(x_1 = 0, x_2)}{\partial x_1} = 0 \tag{18c}$$

$$q_{x1} = \frac{\partial T(x_1 = W, x_2)}{\partial x_1} = 0 \tag{18d}$$

with

$$T_0 = 100^\circ \mathrm{C} \tag{18e}$$

The insulated boundary condition along the crack surface is specified as

$$q_{x_2} = \frac{\partial T(x_1, x_2)}{\partial x_2} = 0, \quad \text{for } W/2 - a \le x_1 \le W/2 + a \text{ and } x_2 = L/2 \tag{19}$$

The plate is uniformly discretized by considering the grid spacing of $\Delta = L/100$ leading to 10000 material points. Each point has a horizon size of $\delta = 3\Delta$. As shown in Figure 8, a discontinuous temperature distribution occurs along the crack length. Due to the presence of the crack, the horizontal and vertical the heat fluxes concentrates at the crack tips as shown in Figure 9. These behaviors can be succesfully captured by the PDDO.

Comparisons of the PD temperature and heat flux variations with those of ANSYS predictions near the crack tip are presented in Figure 10.

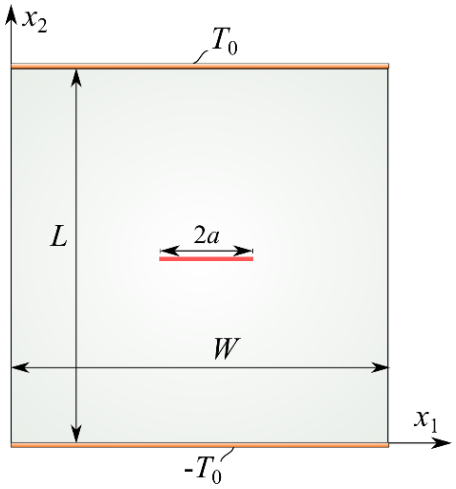


Figure 7. The plate with an insulated crack under temperature boundary conditions.

The PD temperature and heat flux predictions are in good agreement with those obtained from ANSYS predictions. Also, the singularities at the crack tip can be successfuly captured by using PD analysis.

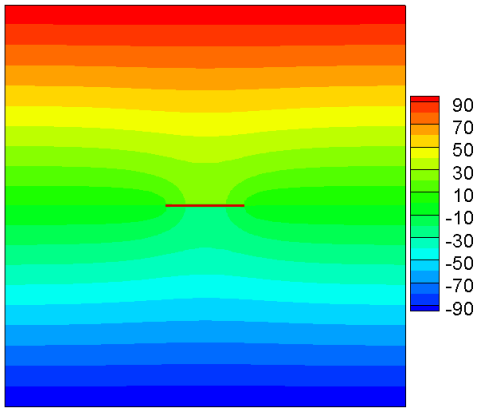
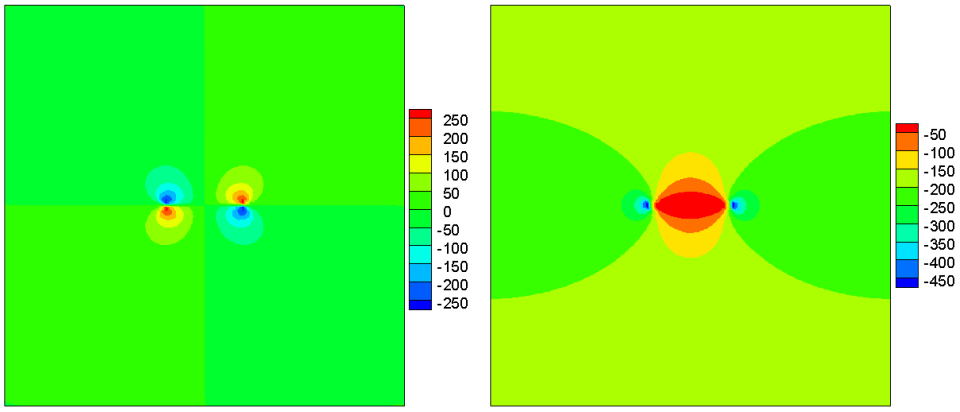
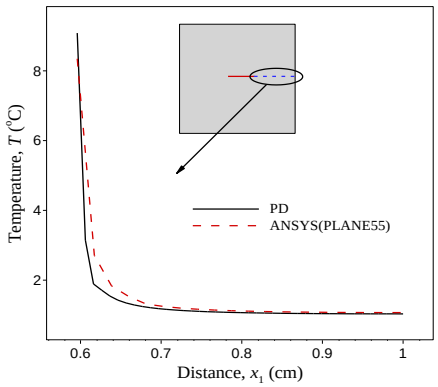


Figure 8. The PDDO temperature, $T(x_1, x_2)$ (°C), predictions for the plate with an insulated crack.

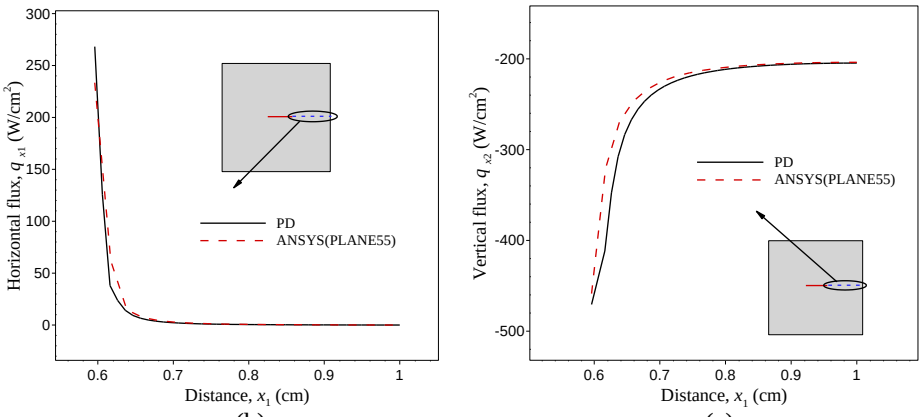


(a) (b)

Figure 9. PD predictions for the heat flux distributions: (a) horizontal flux , $q_{x1}(x_1, x_2)$ (W/cm^2), and (b) vertical flux, $q_{x2}(x_1, x_2)$ (W/cm^2).



(a)



(b) (c)

Figure 10. Comparisons of the PD temperature and heat fluxes with ANSYS results near the crack tip : (a) Temperature $T(^\circ\mathrm{C})$, (b) horizontal flux $q_{x1}(\mathrm{W/cm^2})$, and (c) vertical flux $q_{x2}(\mathrm{W/cm^2})$.

5.3. Plates with Multiple İnsulated Cracks Under Temperature Boundary Conditions

In order to demonstrate the capability of the PDDO, two plates with multiple cracks are considered under temperature boundary conditions. The plate geometry is the same as specified previously. The temperature boundary conditions are imposed on top and bottom edges of both plates while their remaining edges are insulated. Therefore, the boundary conditions for both plates are specified as

$$T(x_1, x_2 = 0) = -T_0 \tag{20a}$$

$$T(x_1, x_2 = L) = T_0 \tag{20b}$$

$$q_{x1} = \frac{\partial T(x_1 = 0, x_2)}{\partial x_1} = 0 \tag{20c}$$

$$q_{x1} = \frac{\partial T(x_1 = W, x_2)}{\partial x_1} = 0 \tag{20d}$$

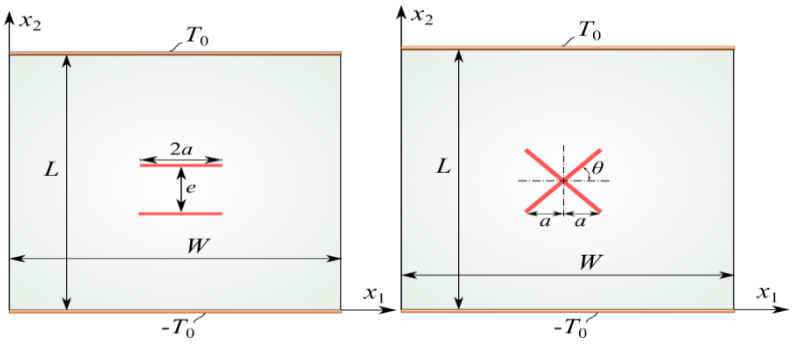
with

$$T_0 = 100^\circ\mathrm{C} \tag{20e}$$

As shown in Figure 11a (Case-I), the insulated cracks are horizontally parallel to each other at the center of the plate having a distance of $e = 0.2$ cm. The length of each crack is specified as $2a$= 0.2 cm.

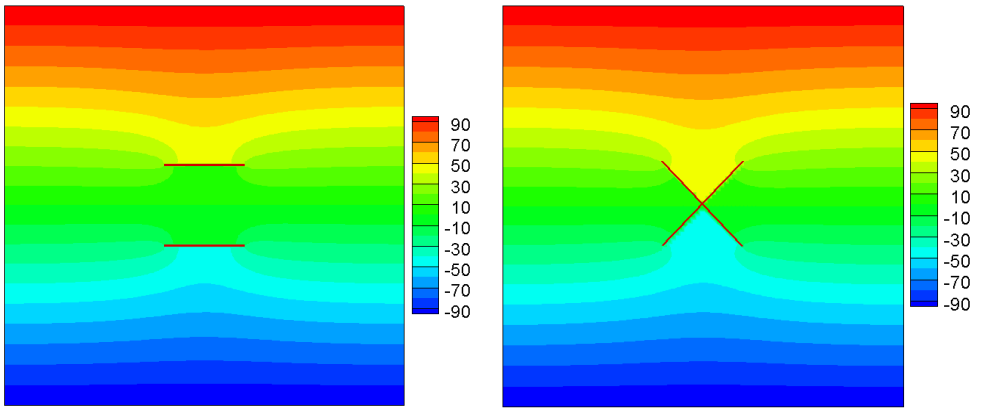
In the second problem (Case-II), the plate consists of two insulated inclined and interacting cracks with a crack orientation of $\theta = 45^\circ$ as shown in Figure 11b. The distance between the crack tips is a= 0.1 cm.

Both plates are uniformly discretized with the grid spacing of $\Delta = L/100$. The family of each grid point is constructed by the horizon size of $\delta = 3\Delta$.



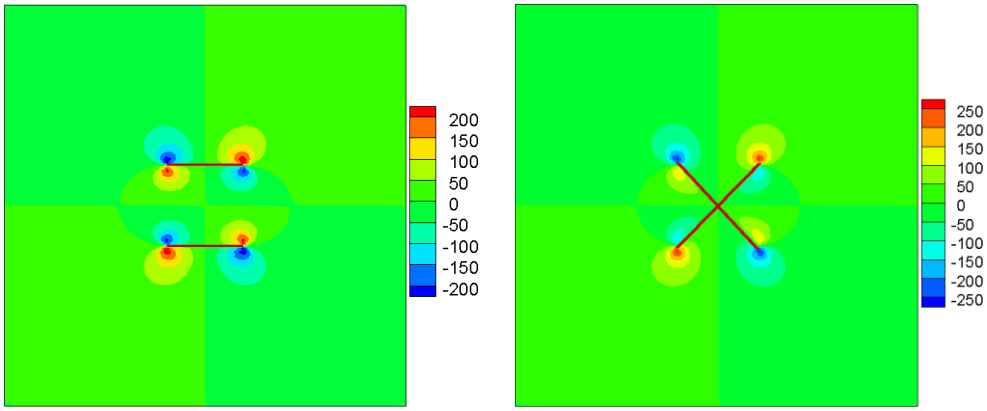
(a) Case-I (b) Case-II

Figure 11. (a) The plate with horizontally parallel insulated cracks, (b) the plate consists of two insulated inclined and interacting crack.



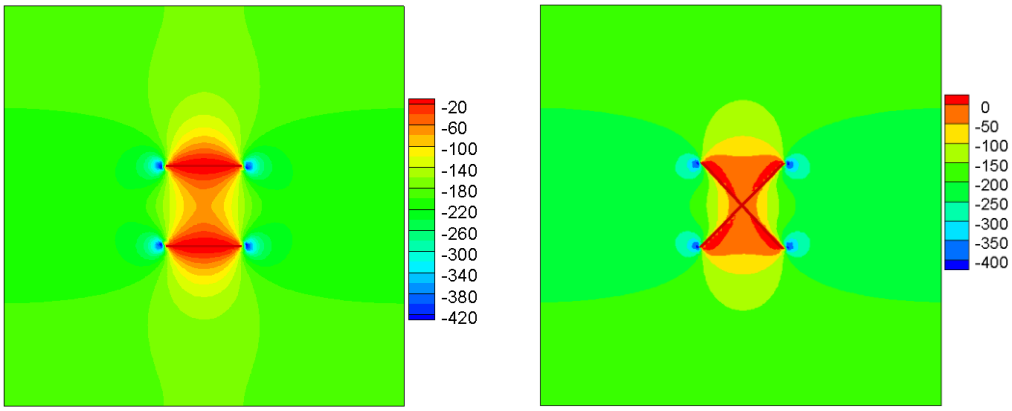
(a) Case-I (b) Case-II

Figure 12. Temperature, $T(x_1, x_2)$ $(^{\circ}\mathrm{C})$, distributions of the plates with insulated cracks under temperature boundary conditions: (a) Case-I and (b) Case-II.



(a) Case-I (b) Case-II

Figure 13. PD predictions for the horizontal heat flux, $q_{x1}(x_1, x_2)$ $(\mathrm{W/cm^2})$, distributions: (a) Case-I and (b) Case-II.



(a) Case-I (b) Case-II

Figure 14. PD predictions for the vertical heat flux, $q_{x2}(x_1, x_2)$ $(\mathrm{W/cm^2})$, distributions: (a) Case-I and (b) Case-II.

Figures 12-14 show the distributions of the temperature $T(x_1, x_2)$, horizontal $q_{x1}(x_1, x_2)$ and vertical $q_{x2}(x_1, x_2)$ heat fluxes in both plates. As observed in these figures, it is obvious that the presence of the cracks exhibits discontinuous temperature fields. Figure 12 shows the temperature values between two parallel cracks drop suddenly because the insulated cracks behave as a thermal barrier in the Case-I problem. In the second problem, X-like crack can be clearly seen in the temperature field. It is apparent that the shielding effect induced by connecting the insulating cracks is correctly captured by the PD solution. The determination of the heat fluxes becomes challenging if the solution domain has a discontinuity such as crack due to the spatial derivaties of the temperature field. As can be seen Figures 13-14, the expected horizontal and vertical flux fields can be captured by the PDDO. In order to compare the temperature and heat flux variations near the crack tip, two problems are also solved by using PLANE55 element of ANSYS with 3710 elements. It is obvious that both PD temperature and heat flux predictions corralete well with those of ANSYS results (Figure 15). It is worth noting that the singular behavior of the heat fluxes are predicted accurately without having any oscillation by PDDO.

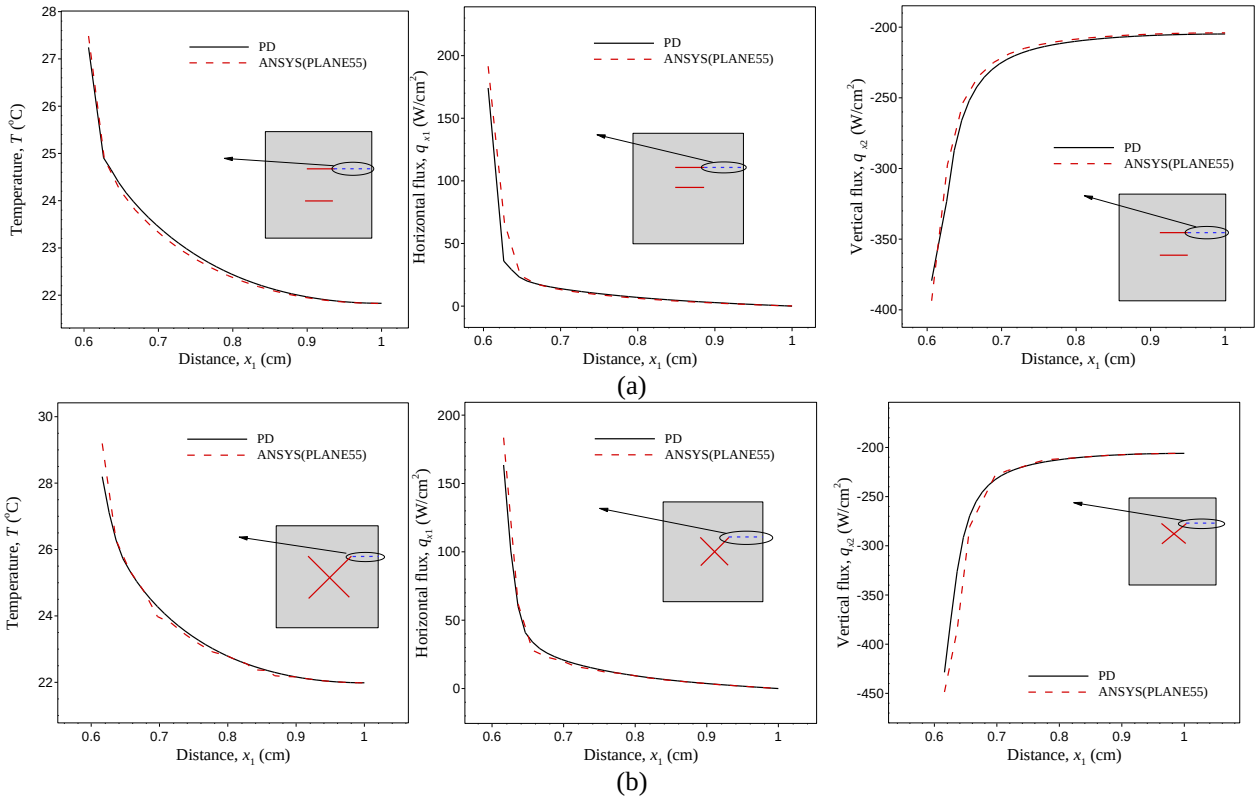


Figure 15. Comparisons of the PD temperature, $T\ (^{\circ}\mathrm{C})$, horizontal q_{x1} $(\mathrm{W/cm^2})$, and vertical q_{x2} $(\mathrm{W/cm^2})$, heat flux variations with ANSYS results near the crack tips: (a) Case-I and (b) Case-II.

6. CONCLUSIONS

This study presents the implementation of PDDO for solving the steady-state heat conduction problems in plates with/without cracks. Generally, the problems consist of discontinuities such as cracks in the solution domain are not easy to consider with a classical treatment due to complications arising from the spatial of derivatives. Since the PD differential operator expresses the nonlocal form of local differential equations, it provides a way to obtain the solution of heat conduction equation in a unified manner regardless of the presence of discontinuities such as cracks. The accuracy and capability of the present approach are demonstrated by considering a plate without cracks. The PD temperature and heat fluxes are evaluated a specified location and compared with the analytical solutions and PLANE55 element of ANSYS predictions. It was observed that the PDDO predictions were in good agreement with both analytical and ANSYS results. Also, the influences of the grid spacing and the size of the horizon on the temperature were investigated by measuring the relative errors between the PD predictions

and analytical solution. The PD estimations converge to the local solutions with decreasing the horizon size.

The cracks in the structural components may result in intensified heat flux concentrations near the crack tips leading to catastrophic failures. Therefore, the temperature and heat flux distributions of the structures should be well understood for their structural integrity. In order to demonstrate the applicability of the present approach, three challenging problems with crack(s) were considered under thermal loads. It was shown that PDDO can easily deal with the problems including a single and multiple cracks. The PD temperature and heat flux variations near the crack tip were compared with the ANSYS results. The PD predictions indicated a good agreement with those of ANSYS.

Coupling between the mechanical and thermal PD models are planned for the future to investigate damage nucleation and growth in the structures. Solidification and melting processes are important and can be applied to phase change or moving interface problems. Hence, the capability of the PDDO on the solution of the solidification and melting problems will be studied in the future.

7. REFERENCES

[1] G. C. Sih, "Heat Conduction in the Infinite Medium With Lines of Discontinuities," *J Heat Trans*, Vol. 87, pp. 293-298, 1965.

[2] W. H. Chen and C. L. Chang, "Heat Conduction Analysis of a Plate With Multiple İnsulated Cracks by the Finite Element Alternating Method," *Int J Solids Struct*, Vol. 31, pp. 1343-1355, 1994.

[3] W. H. Chen and C. L. Chang, "Analysis of Two-Dimensional Mixed Mode Crack Problems by Finite Element Alternating Method," *Comput Struct*, Vol. 33, pp. 1451-1458, 1989.

[4] W. H. Chen and C. L. Chang, "Analysis of Two-Dimensional Fracture Problems with Multiple Cracks Under Mixed Boundary Condition," *Eng Fract Mech*, Vol. 34, pp. 921-934, 1989.

[5] S. Li and W. K. Liu, "Meshfree Particle Methods," *Springer*; 2004.

[6] G. D. Mahan and F. Claro, "Nonlocal Theory of Thermal-Conductivity," *Phys Rev B*, Vol. 38, pp. 1963-1969, 1998.

[7] G. Lebon and M. Grmela, "Weakly Nonlocal Heat Conduction in Rigid Solids," *Phys Lett A*, Vol. 214, pp. 184-188, 1996.

[8] W. Gerstle, S. Silling, D. Read, V. Tewary and R. Lehoucq, "Peridynamic Simulation of Electromigration," *Comput Mater Continua*, Vol. 8, pp. 75-92, 2008.

[9] F. Bobaru and M. Duangpanya, "The Peridynamic Formulation for Transient Heat Conduction," *Int J Heat Mass Transf*, Vol. 53, pp. 4047-4059, 2010.

[10] E. Madenci and E. Oterkus, "Peridynamic Theory and Its Applications," *Springer*, 2014.

[11] E. Madenci , A. Barut and M. Dorduncu, "Peridynamic Differential Operator for Numerical Analysis," *Springer*, 2019.

[12] S.A. Silling, "Reformulation of Elasticity Theory For Discontinuities and Long-Range Forces,". *J Mech Phy Solids*, Vol. 48, pp. 175-209, 2000.

[13] S.A. Silling, M. Epton, O. Weckner, J. Xu, and E. Askari, "Peridynamic States and Constitutive Modeling," *J Elast*, Vol. 88, pp.151-184, 2007.

[14] M.N. Ozisik, "Heat Conduction," *Wiley*, 1980.

VITAE

Mehmet Dördüncü received his PhD in Mechanical Engineering in 2018 from University of Arizona. He worked as a research assistant in the Department of Aerospace and Mechanical Engineering at the University of Arizona during his PhD studies. He was a visiting student at Nasa Langley Research Center (2016), Hampton, VA, where he conducted research on the development of Refined Zigzag Theory for predicting failure in composite structures. He is the co-author of Peridynamic Differential Operator for Numerical Analysis (Springer, 2019). His current research is mainly focused on computational mechanics of materials and structures by using peridynamics, peridynamic differential operator, and finite element method. He is currently a faculty member in the Department of Mechanical Engineering at Erciyes University, Kayseri.